Supporting Information

Muraro et al. 10.1073/pnas.1221766111

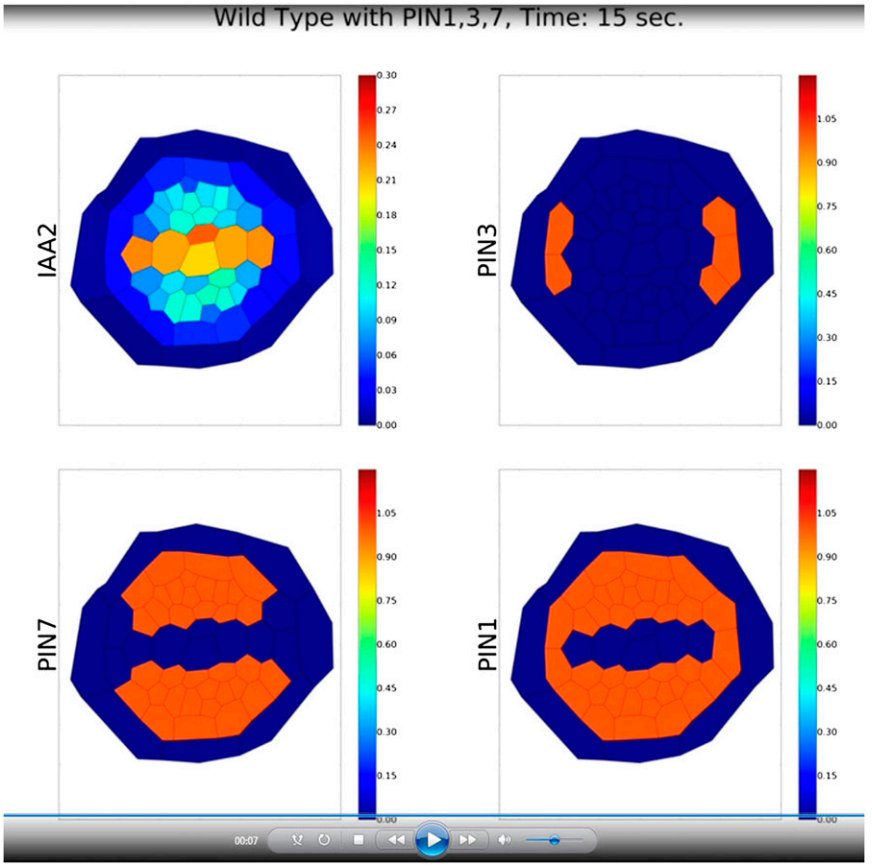

Movie S1. Simulation of *IAA2* expression when PIN1, PIN3, and PIN7 are active. Auxin is actively transported into the xylem axis, where it forms a maximum and activates the expression of *IAA2*. The parameters associated with cytokinin and all parameters of transcription and translation have been set to zero, except those parameters relating to *IAA2* expression. PIN1, PIN3, and PIN7 concentrations have been set to unity. The other parameters have been set to the values reported in *SI Appendix*, Tables S2 and S3.

Movie S1

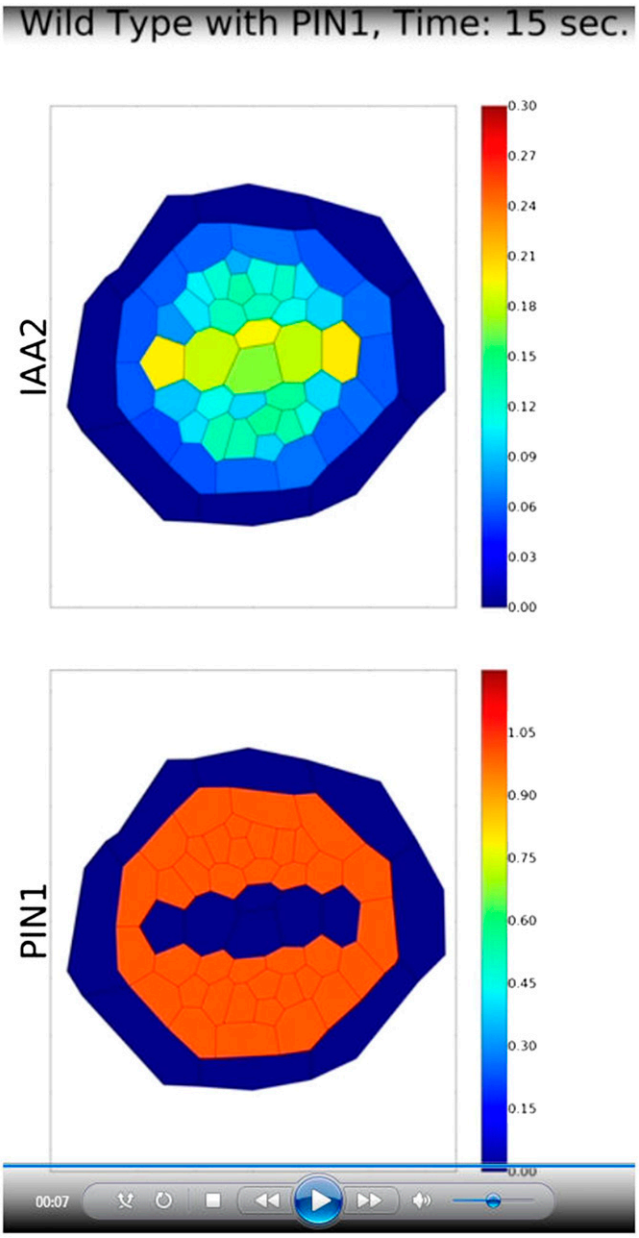

Movie S2. Simulation of *IAA2* expression when only PIN1 is active. PIN1 is sufficient to reproduce the auxin signaling maximum seen in WT plants. The parameters associated with cytokinin and all parameters of transcription and translation have been set to zero, except for those parameters relating to *IAA2* expression. The PIN1 concentration has been set to unity. The other parameters have been set to the values reported in *SI Appendix*, Tables S2 and S3.

Movie S2

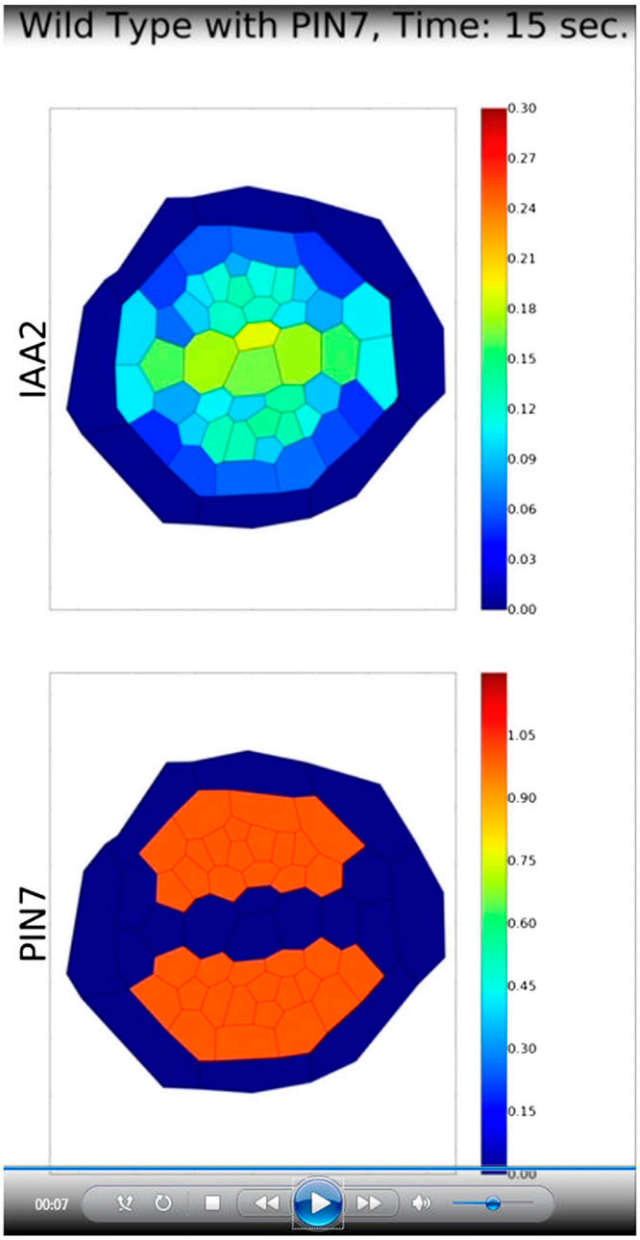

Movie S3. Simulation of *IAA2* expression when only PIN7 is active. PIN7 acts redundantly with PIN1 to direct the auxin signaling maximum. The parameters associated with cytokinin and all parameters of transcription and translation have been set to zero, except for those parameters relating to *IAA2* expression. The PIN7 concentration has been set to unity. The other parameters have been set to the values reported in *SI Appendix*, Tables S2 and S3.

Movie S3

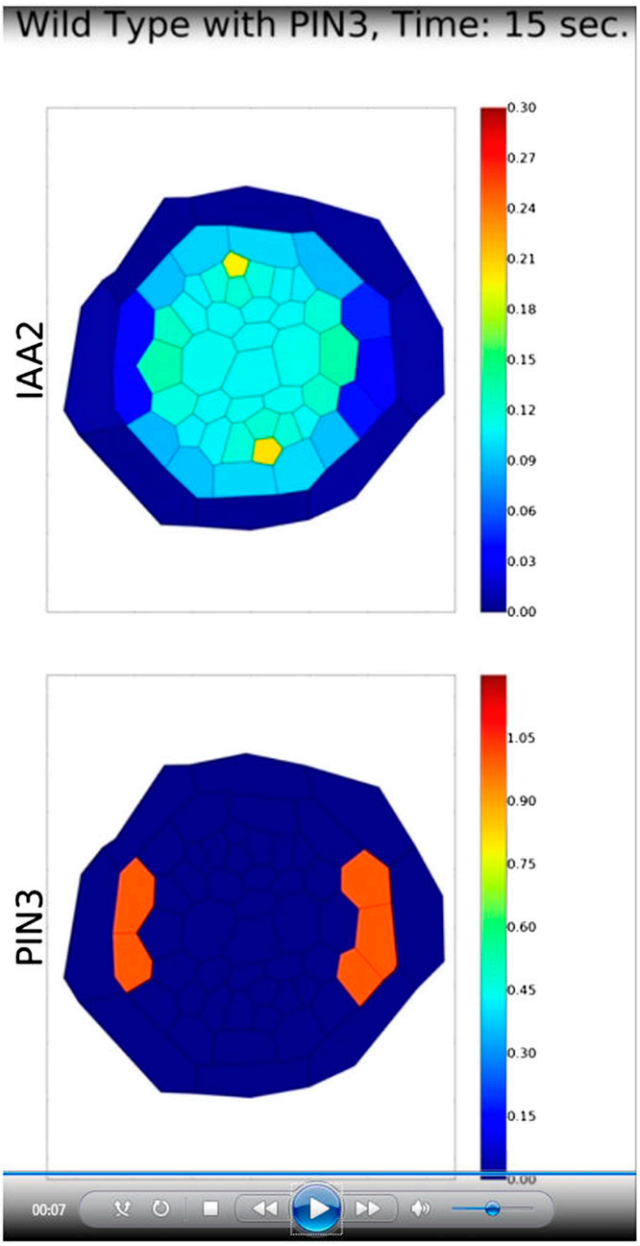

Movie S4. Simulation of *IAA2* expression when only PIN3 is active. PIN3 activity alone is insufficient to reproduce the auxin signaling maximum seen in WT plants. The parameters associated with cytokinin and all parameters of transcription and translation have been set to zero, except for those parameters relating to *IAA2* expression. The PIN3 concentration has been set to unity. The other parameters have been set to the values reported in *SI Appendix*, Tables S2 and S3.

Movie S4

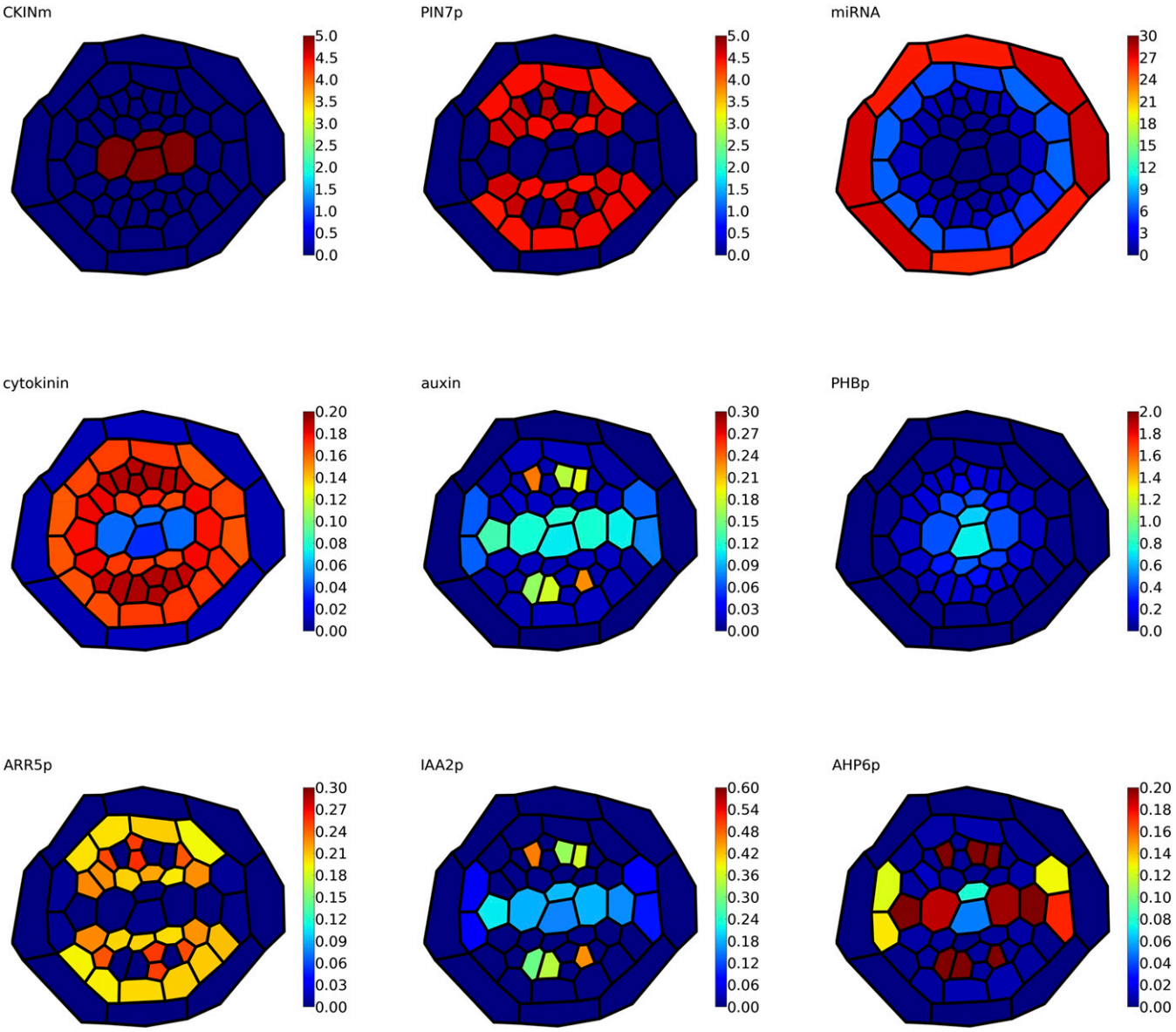

Movie S5. Simulation of our multicellular model of vascular patterning with all known network components active. In this simulation, there is no mutual degradation present between *PHABULOSA* (*PHB*) mRNA and microRNA165/6 (miRNA165/6). As a consequence, the simulation fails to generate a sharp gradient of *PHB*, which results in altered expression of *AHP6*. All parameters have been set to their default values, which are reported in *SI Appendix*, Tables S2 and S3, except for $pCKIN_m$ and $d_{miRNA/mRNA}$, which have been set to zero.

Movie S5

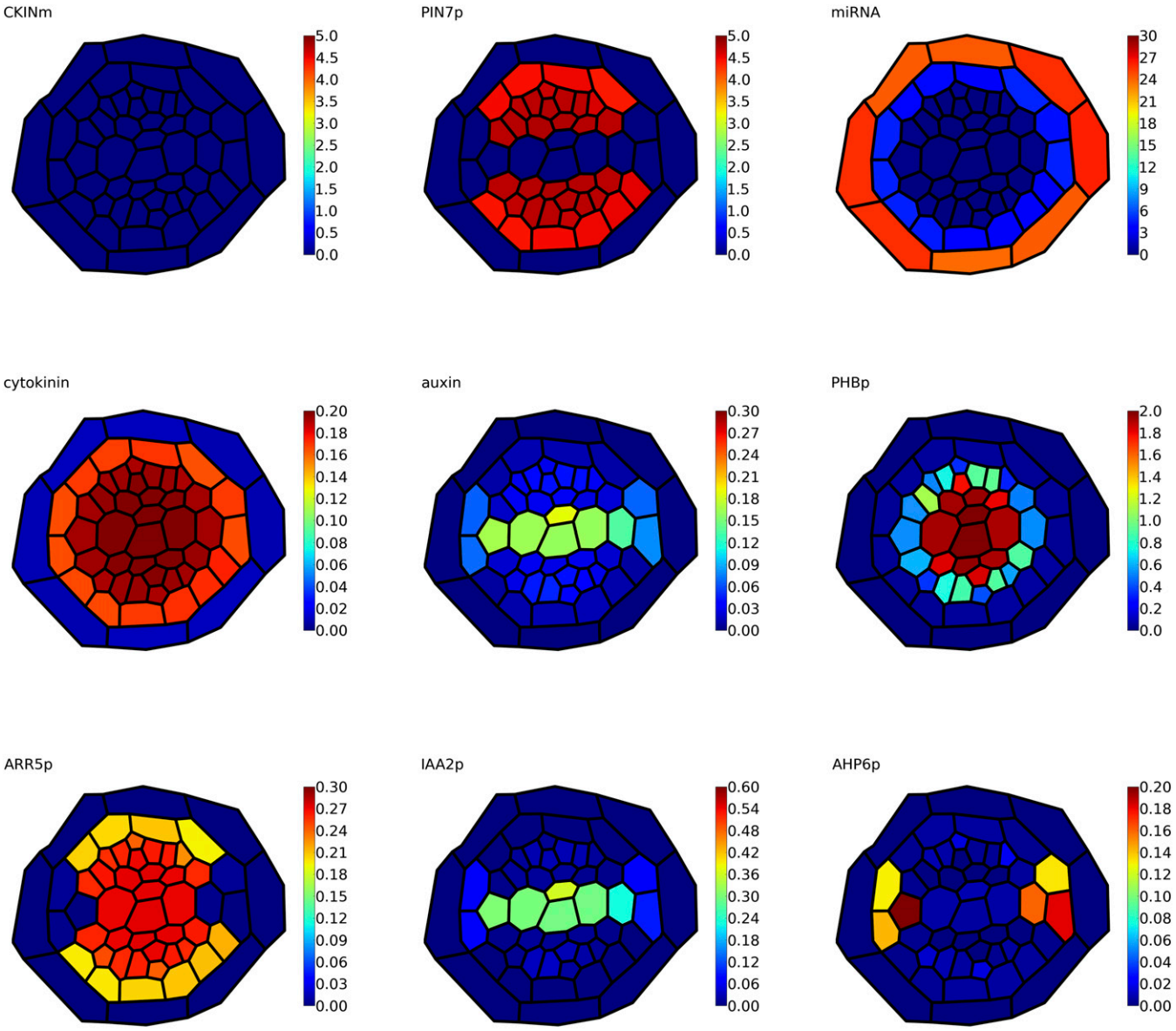

Movie S6. Simulation of our multicellular model of vascular patterning with all known network components active and incorporating the mutual degradation between *PHB* mRNA and miRNA165/6. This simulation is able to recapitulate the experimentally observed gradient of *PHB* expression, and the simulated patterns of all components are in agreement with the experimental observations except for ARR5, where the simulated expression is also present in the metaxylem. All parameters have been set to their default values, which are reported in *SI Appendix*, Tables S2 and S3, except for $pCKIN_m$, which has been set to zero.

Movie S6

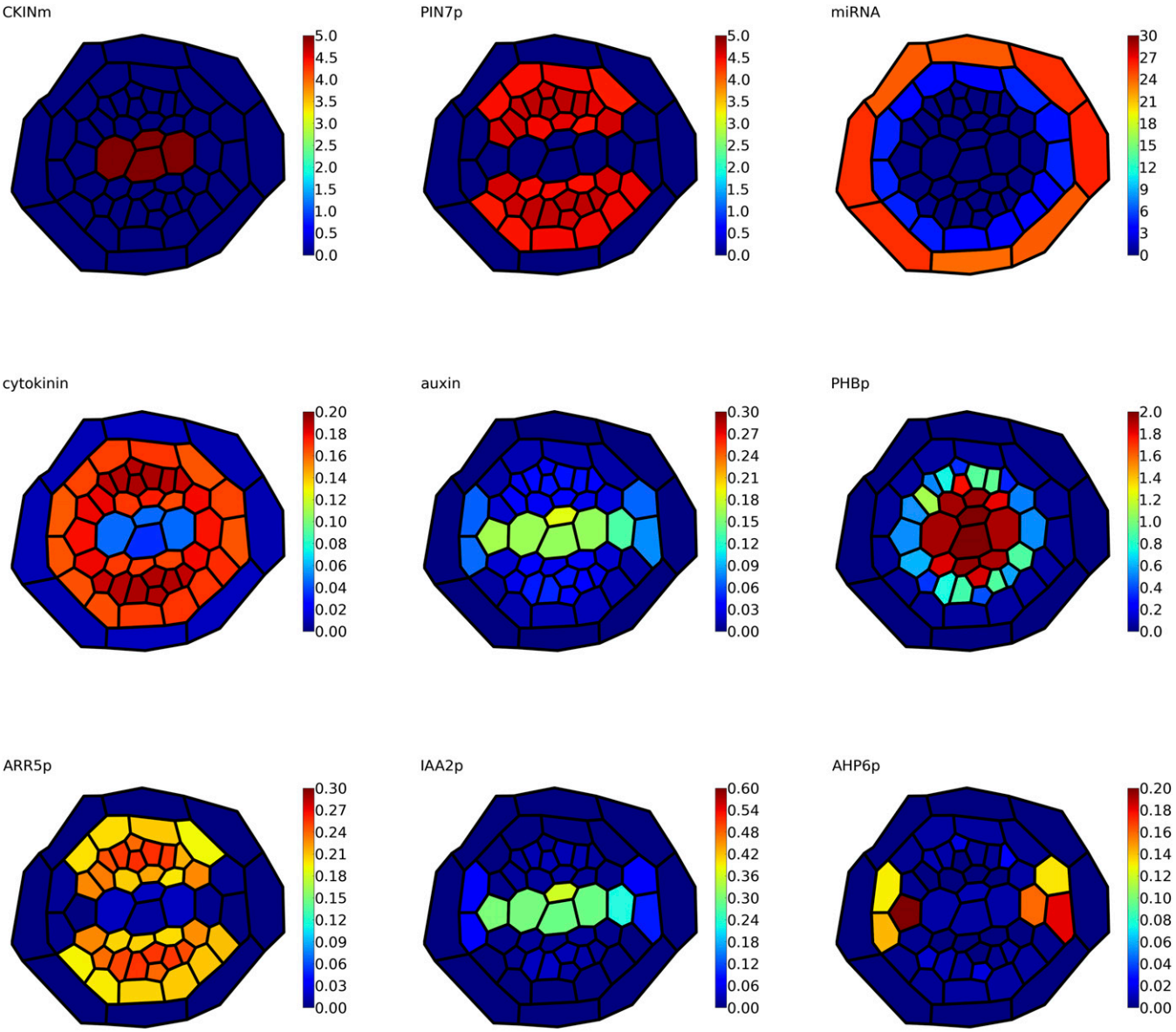

Movie S7. Simulation of our multicellular model of vascular patterning with a cytokinin inhibitor (CKIN) present in the metaxylem. Inclusion of a cytokinin inhibitor into our model with constitutive expression in the metaxylem degrades cytokinin levels, and *ARR5* expression becomes similar to experimental observations. All parameter shave been set to the values reported in *SI Appendix*, Tables S2 and S3.

Movie S7

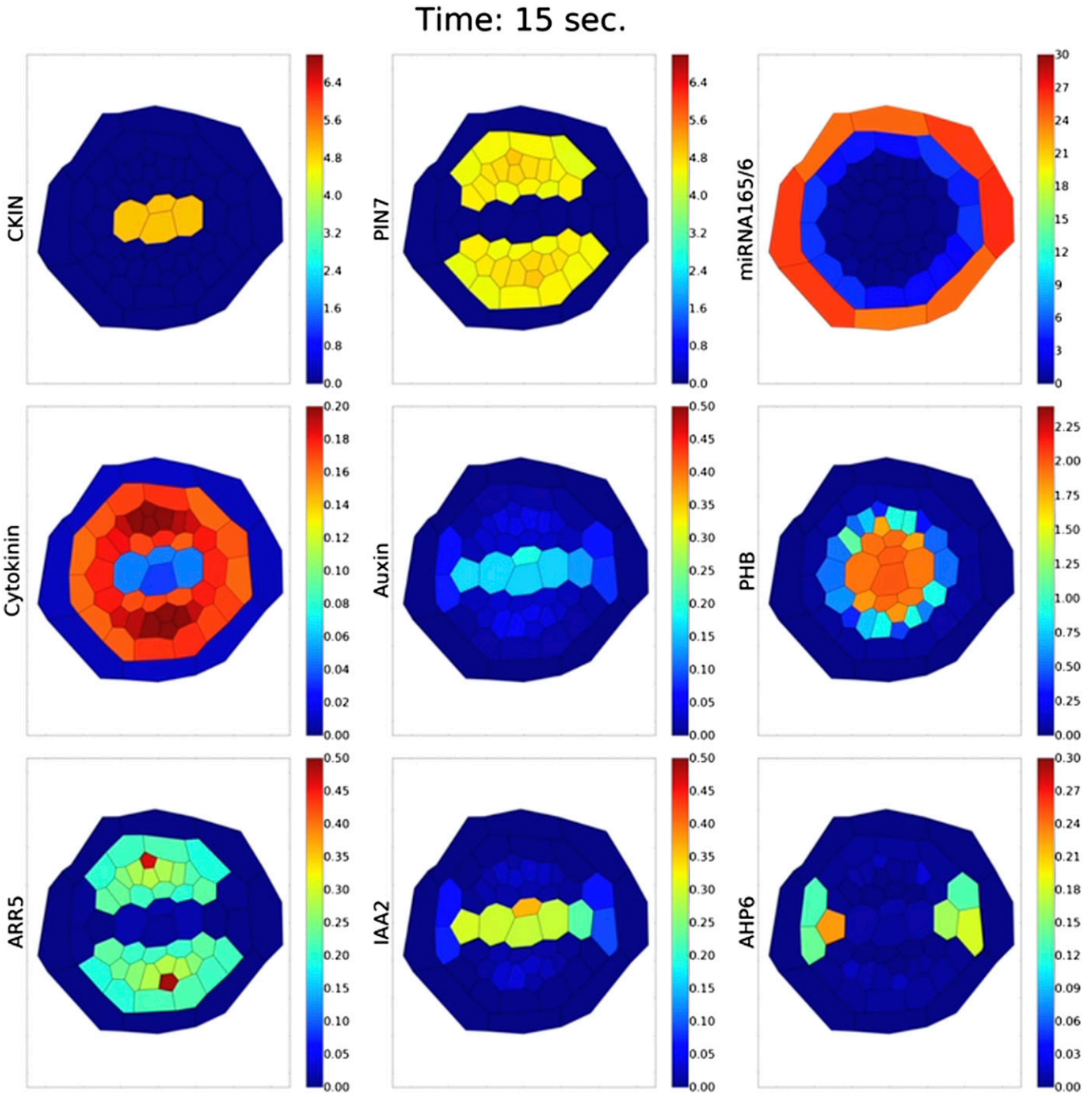

Movie S8. Simulation of our multicellular model of vascular patterning, in which the phloem is specified as the main source for cytokinin. Specifying the phloem as the main source of cytokinin causes an uneven gradient of *ARR5* response. We do not observe this uneven response pattern in our experimental analyses. These simulations suggest that a positional bias in the input of hormones is not required. The parameters have been set to the values reported in *SI Appendix*, Tables S2 and S3, except for the biosynthesis rate for cytokinin p_{Ck} in the phloem, which was set to two times its default value.

Movie S8

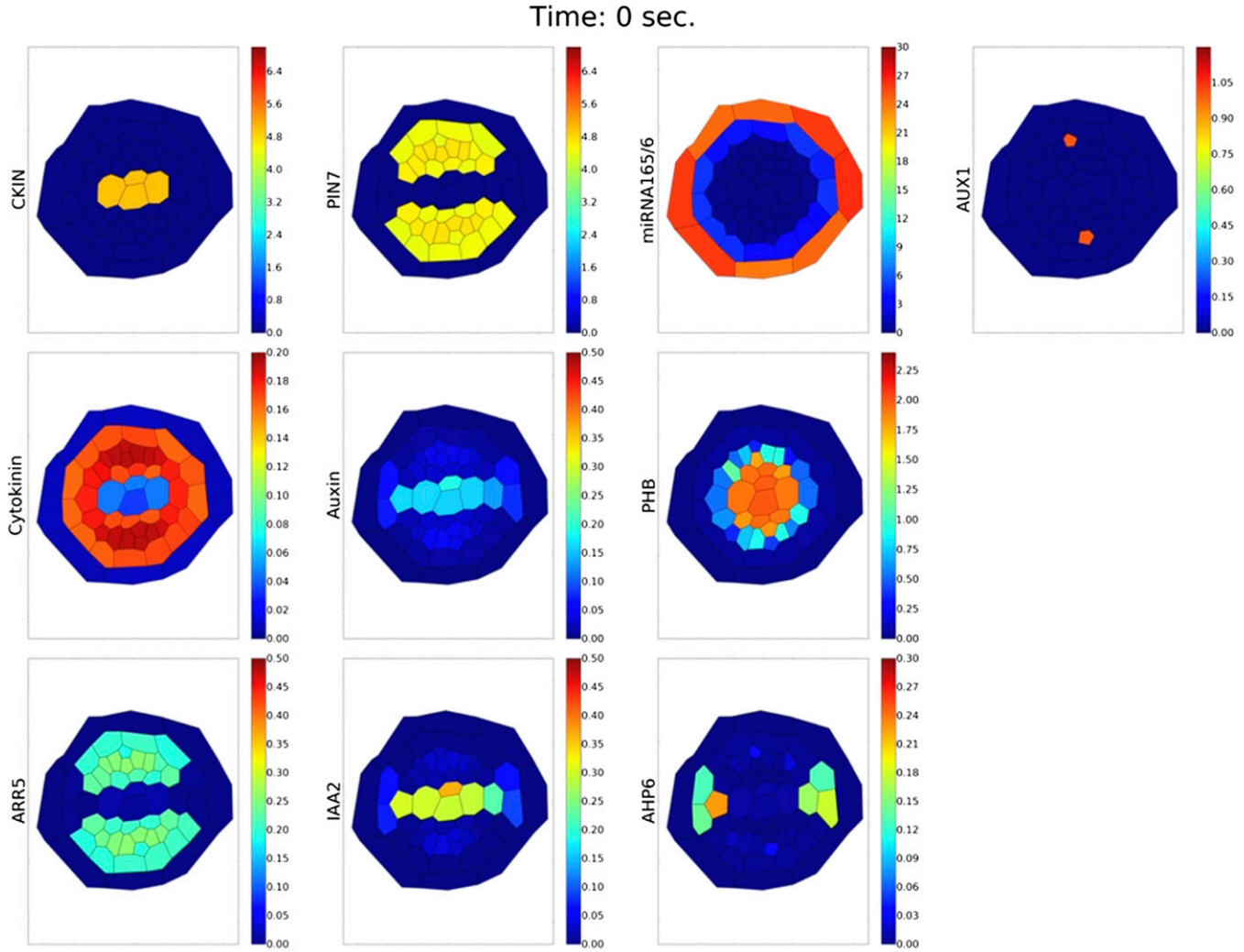

Movie S9. Simulation of our multicellular model of vascular patterning containing a phloem-localized auxin influx carrier, AUX1. AUX1 is modeled as a PIN in the inverse direction (influx instead of efflux) with the same transport rate as for the PINs ($T_{AUX1} = T_{Aux} = 20.0$ μm μM^{-1} s^{-1}). AUX1 is localized on all of the membranes of the phloem cells and constantly expressed in the phloem, its unitary concentration being proportionally divided on the cell walls. The inclusion of such a component has little effect on the overall expression of the reporter genes. All parameters have been set to the values reported in *SI Appendix*, Tables S2 and S3.

Movie S9

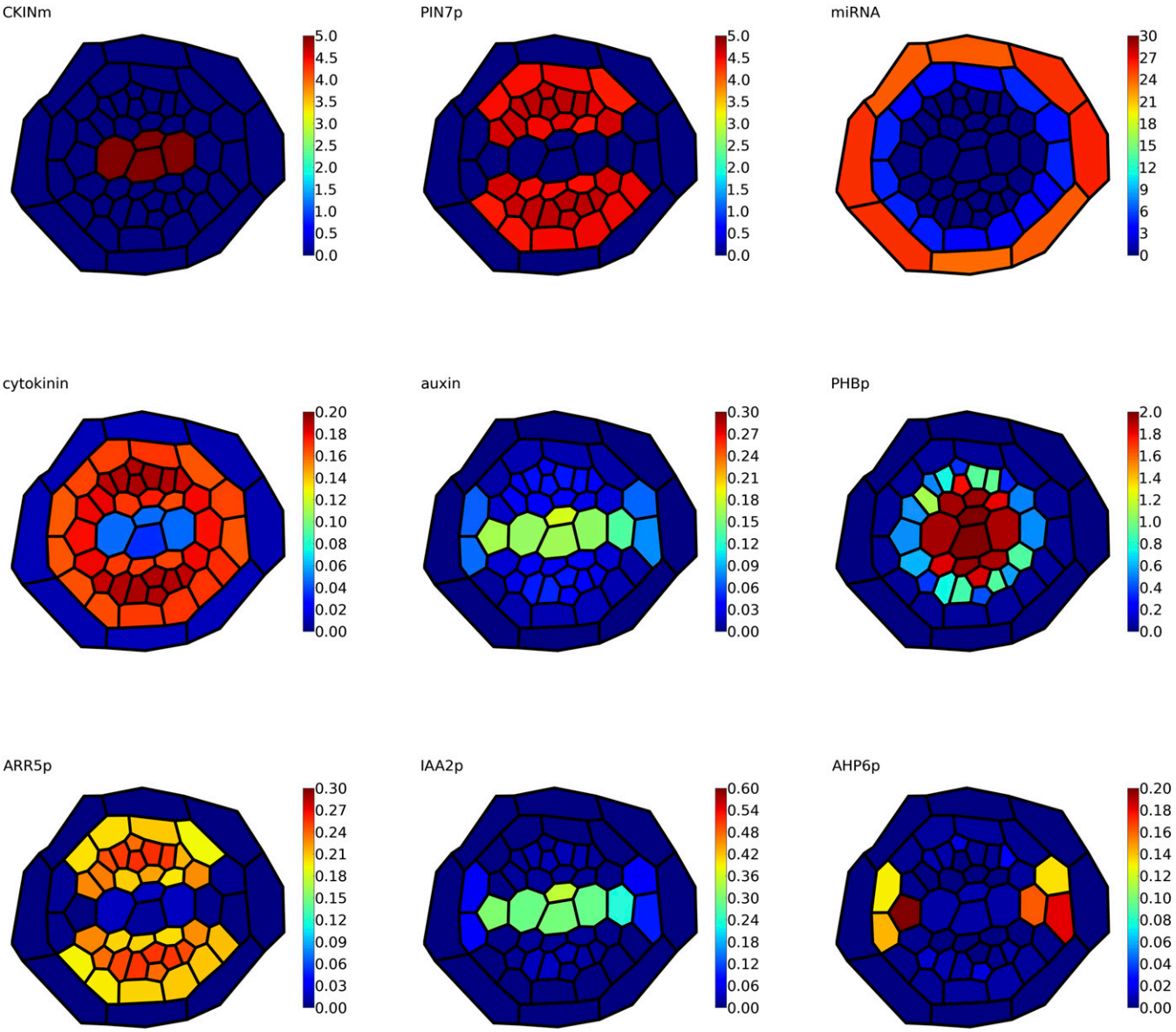

Movie S10. Simulation of our extended model showing the robustness of this genetic network in regulating vascular pattern. In this simulation, the initial conditions relating to the concentration of all network components are set to be equal to the output of simulation SM7 (this distribution of components closely resembles the expression pattern in a WT root). However, all cells are given the potential to express *PIN7*. The interaction between network components in this parameter space is able to robustly maintain the initial conditions.

Movie S10

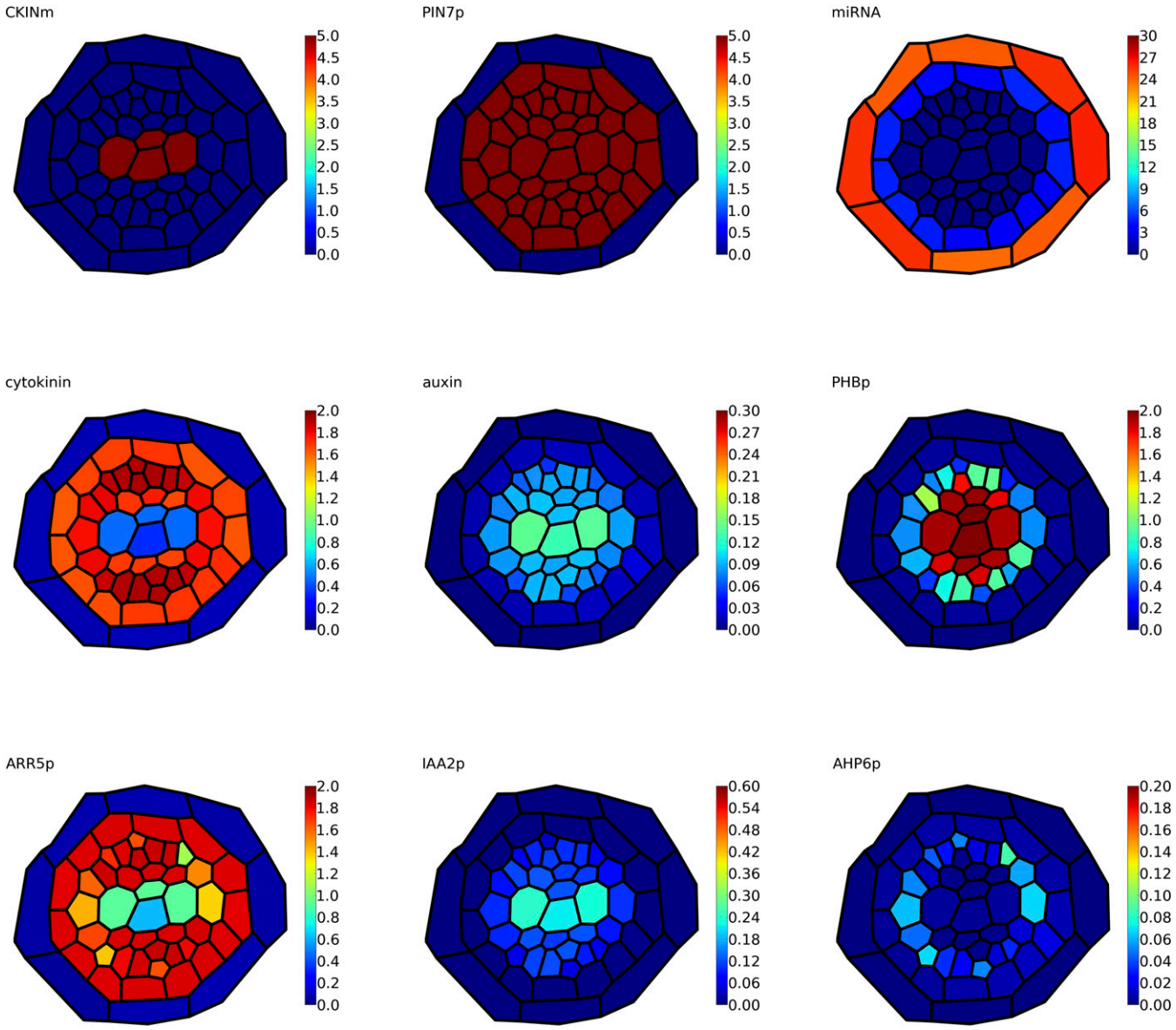

Movie S11. Simulation of our extended model testing the effect of increased cytokinin on vascular patterning. The simulation has been set up using the same initial conditions and parameter set as SM12, except that p_{Ck} has been set to 20.0 $\mu M\ s^{-1}$. Under similar conditions, when exogenous cytokinin has been applied to growing roots, it has been observed that *AHP6* expression is lost and that auxin response becomes restricted to the central cells. Increasing the cytokinin levels in this simulation has a similar affect, indicating that our model has the capacity to repattern and that correct maintenance of cytokinin synthesis within a certain threshold is required to maintain a stable vascular pattern.

Movie S11

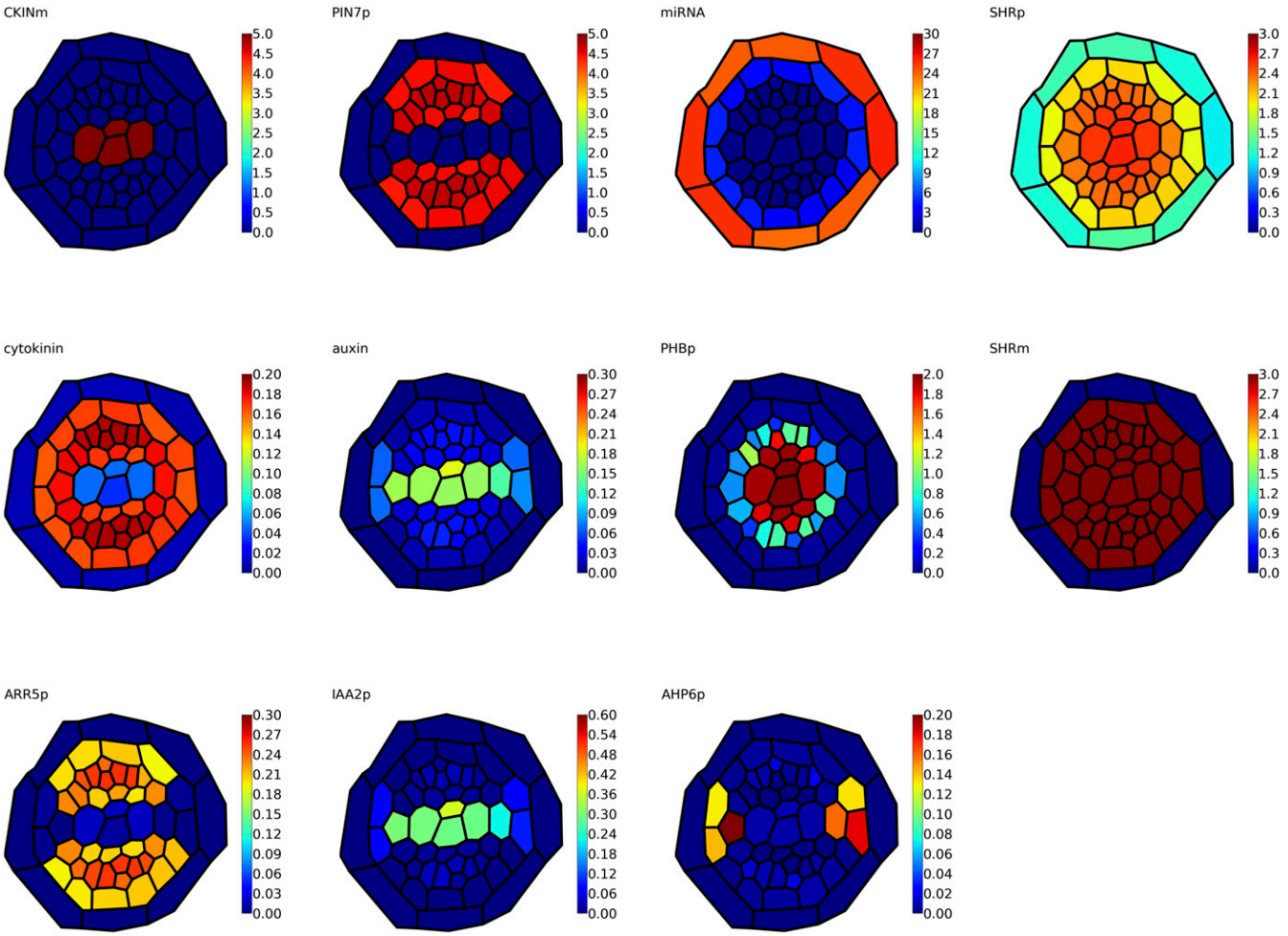

Movie S12. Simulation of our extended multicellular model of vascular patterning incorporating regulation of miRNA165/6 by SHORT ROOT (SHR). All of the other components and PIN distribution are maintained like in SM7. The pattern is maintained when including SHR-dependent regulation of miRNA165/6. The parameters have been set to the values reported in *SI Appendix*, Tables S2, S3, and S11.

Movie S12

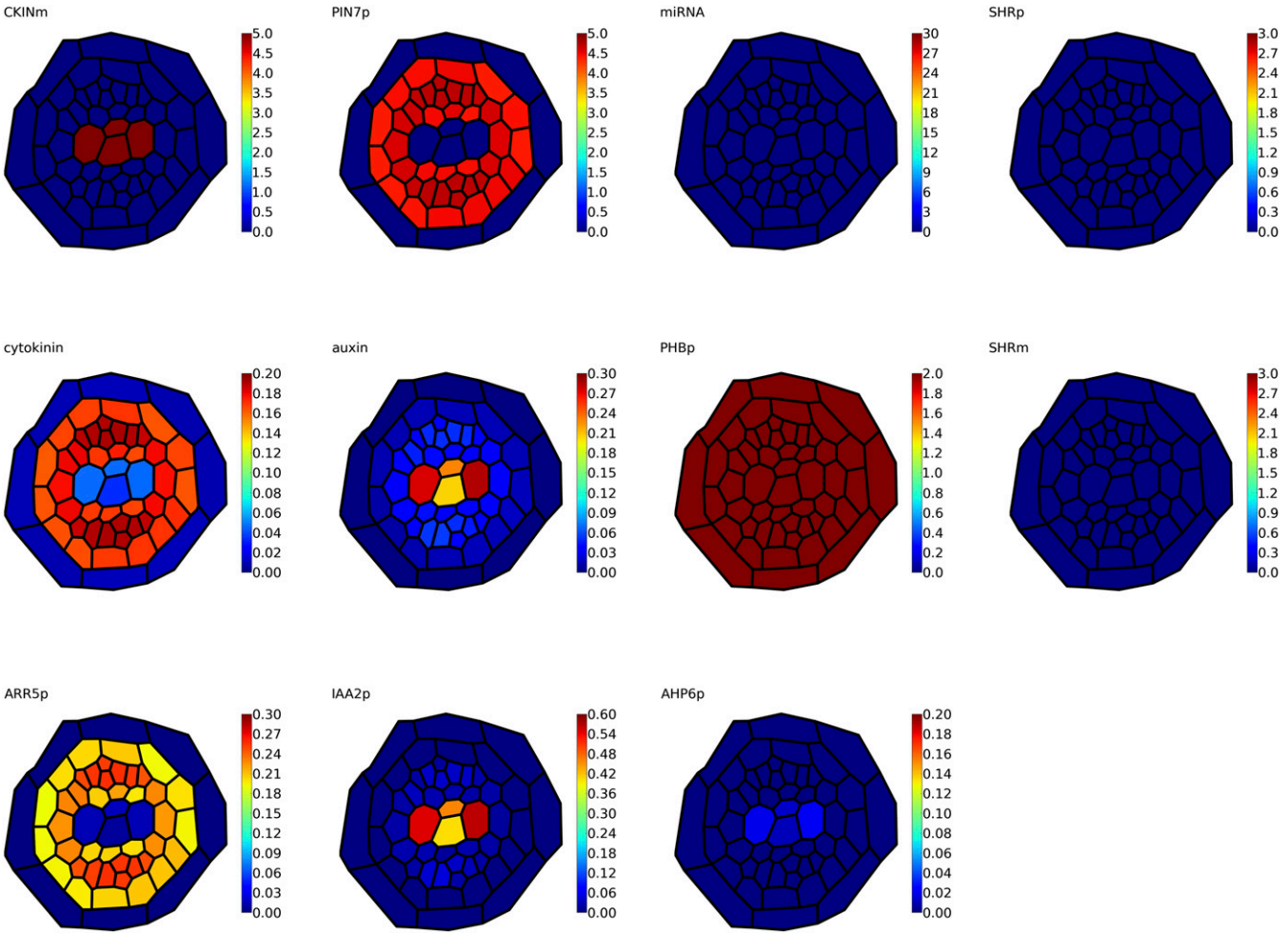

Movie S13. Simulation of our extended model testing the requirement of SHR for establishing the correct hormonal response pattern. The simulation has been set up using the same initial conditions and parameter set as SM12, except that the transcription rate of *SHR* ($pSHR_m$) has been set to zero. Under these conditions, our model predicts a flat field of *PHB* expression. This pattern of PHB results in a reduction in the level of AHP6, an expansion in the domain of *PIN7* so that it becomes approximately radially symmetric, and a restriction in the domain of auxin output to the central cells in the xylem axis.

Movie S13

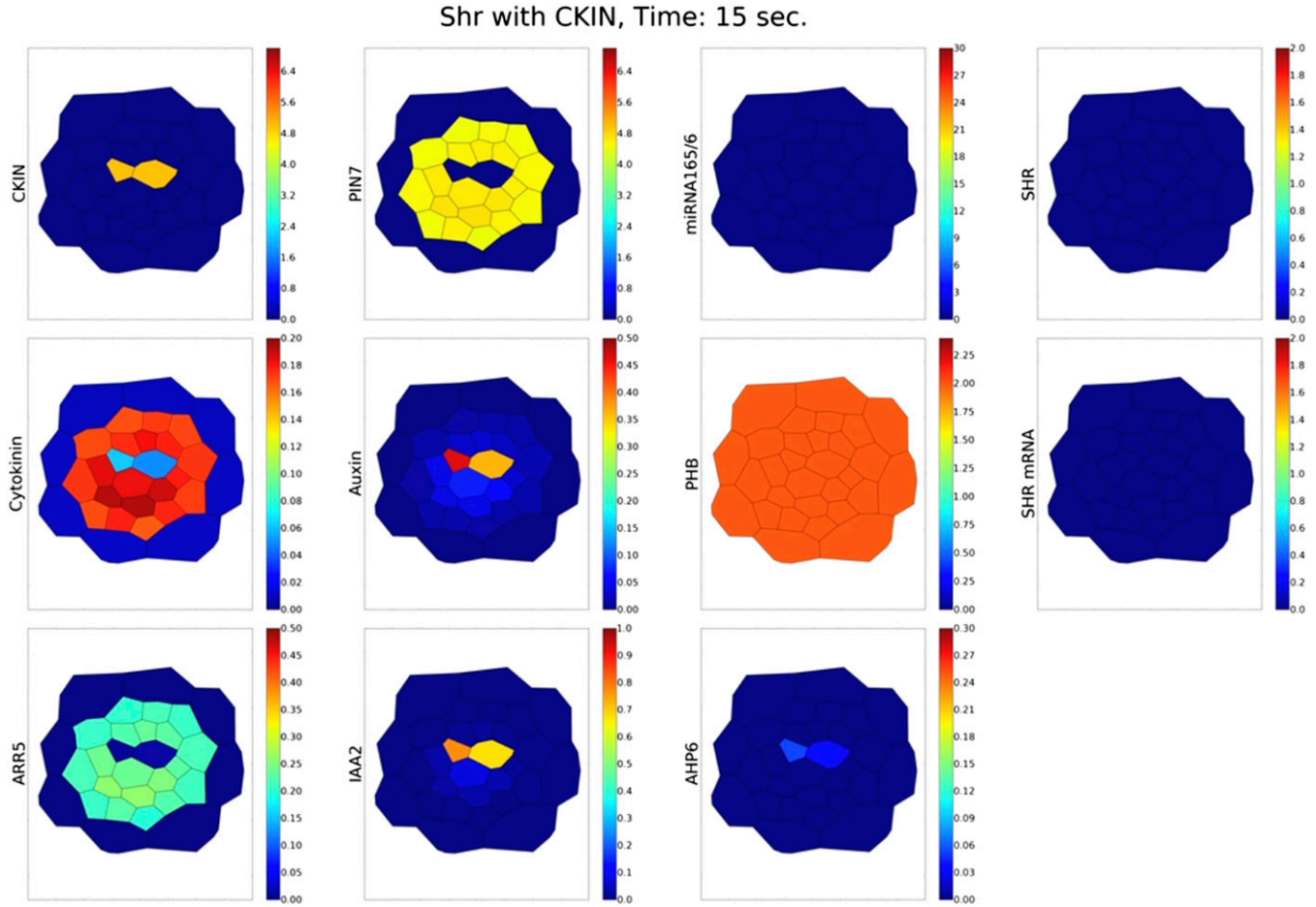

Movie S14. Simulation of our extended multicellular model of vascular patterning in an *shr* mutant. In this simulation, we have used the geometry of an *shr* mutant for the simulations. *IAA2* response is restricted to the metaxylem, whereas *PIN7* is expressed in an expanded, approximately radially symmetric pattern. The parameters have been set to the values reported in *SI Appendix*, Tables S2, S3, and S11, except for $pSHR_m$, which has been set to zero.

Movie S14

Other Supporting Information Files

SI Appendix (PDF)